Mechanical Systems and Signal Processing 155 (2021) 107591

Contents lists available at ScienceDirect

Mechanical Systems and Signal Processing

journal homepage: www.elsevier.com/locate/ymssp

Bloch waves in an array of elastically connected periodic slender structures

Danilo Karličić [a,b], Milan Cajić [a,b,*], Stepa Paunović [b], Sondipon Adhikari [a]

[a] College of Engineering, Swansea University, United Kingdom
[b] Mathematical Institute of the Serbian Academy of Sciences and Arts, Belgrade, Serbia

ARTICLE INFO

Article history:
Received 5 July 2020
Received in revised form 29 November 2020
Accepted 26 December 2020
Available online 21 January 2021

Keywords:
Bloch waves
Galerkin approximation
Band structure
Elastically connected beams
Concentrated masses

ABSTRACT

This paper proposes the methodology to carry out the analysis of Bloch wave propagation in an array of vertically aligned and elastically connected structural elements such as beams, strings, plates, or other slender structures. The suggested approach is based on the Galerkin approximation and Floquet-Bloch theorem used in defining the eigenvalue problem and obtaining the band structure of the periodic systems. Special attention is devoted to the case of elastically connected Rayleigh beams with attached concentrated masses and wave propagation in the direction normal to the beam's length. A validation study is performed by using the finite element model and the frequency response function to confirm the accuracy of the solution obtained via the Galerkin approximation. Two configurations of unit cells, having two and three elastically connected beams with different geometrical and material properties, are considered in the numerical study. The effects of various parameters are investigated to reveal their influence on the frequency band structure and emergence of the zero-frequency bandgap. The results of this study demonstrates the tunability properties of the proposed periodic systems due to changes in values of concentrated masses, stiffness of the coupling medium or boundary conditions on structural elements within the unit cell.

1. Introduction

Some early notable contributions by Mead and co-workers [1] in the field of harmonic wave propagation analysis in periodic structures motivated many researchers. The main attention in those works was given to one-dimensional [2–4] and two-dimensional periodic structures [5]. It is a well-known fact that waves propagating in a homogeneous continuum are non-dispersive. Contrarily, in a heterogeneous structured medium such as beams and plates, dispersion occurs due to the presence of physical boundaries. Another characteristic of heterogeneous medium, which might be the consequence of microstructural properties or structural interfaces, is the existence of bandgaps as frequency intervals at which waves decay exponentially. This implies difference between homogeneous and heterogeneous medium that was demonstrated in [6], where flexural harmonic waves propagating within the bi-coupled periodic system composed of Euler-Bernoulli beams have been analyzed in great detail. The authors have demonstrated that periodicity, which introduces the internal length, causes the dispersion curve to be reflected at the boundary of the first Brillouin zone. This makes it possible to apply the Floquet-Bloch theory and obtain the dispersion relation that allows one to distinguish pass-bands, the frequencies of the waves that

* Corresponding author at: College of Engineering, Swansea University, United Kingdom.
E-mail addresses: milan.cajic@swansea.ac.uk, mcajic@mi.sanu.ac.rs (M. Cajić).

https://doi.org/10.1016/j.ymssp.2020.107591
0888-3270/

propagate without attenuation, and stop-bands (bandgaps) where the waves decay exponentially. However, in that study only the bi-coupled continuous and discrete systems rigidly connected in series and parallel were considered. Here, the main focus is put on specific type of heterogeneous systems composed of an array of parallel and elastically connected periodic slender structures of the same length/width and boundary condition by studying the wave propagation along the array.

A good example of harmonic axial wave propagation in one-dimensional quasiperiodic-generated structured rods was investigated in [7], which is given as an infinite bar with repeated elementary cells designed by using the Fibonacci substitution rules. Propagation of a transition wave in a more complex system composed of a finite heterogeneous discrete beam strip with periodically placed masses and subjected to the harmonic load was investigated in [8]. Some authors devoted special attention to problems of flexural waves propagation in structures resting on elastic foundation due to the relevance of this subject in various engineering applications.These application examples include models of infinite beams on elastic support carrying a dynamic load that represent slabs, rails or road pavements. The effects of compressive load and support's damping on the dispersion characteristic and transient response of a beam lying on elastic foundation of Winkler type is investigated in [9]. A more complex case was studied in [10] by analyzing the wave propagation and attenuation properties in ordered and disordered periodic composite beams on elastic foundations due to moving loads. It has been shown that one-dimensional discrete flexural systems composed of massless beams connecting periodically placed masses can be used to approximate the Rayleigh's beam on elastic foundation in the long-wavelength limit [11]. In [12], the authors investigated the existence of localized modes in a set of quasi-periodic continuous elastic beams with attached array of ground springs. It is shown that vibration modes are first localized at a boundary and then migrate into a bulk for a varied projection parameter. The structured Rayleigh beams on the elastic foundation that can exhibit dispersion wave characteristics and localized wave-forms were analysed in [13]. Moreover, the influence of pre-stress on the bandgap formation of the elastic beam on elastic foundation was studied in [14]. The authors introduced repeated elementary cells generated by adopting the Fibonacci sequence and then solved the eigenvalue problem by using the transmission matrix of the unit cell and the Bloch solution. By considering the Rayleigh beam theory, the free and forced wave propagation in an elastic grid structure was analysed in [15], where several forms of vibration localization and wave channeling were observed. It was demonstrated that the localization is triggered by several parameters such as rotation inertia and external excitation. By considering the complex beam model suggested in [16], an energy harvesting device was developed based on the metamaterials design, showing great applicability in surface wave control.

Most of the wave dispersion analyses of two-dimensional multi-structural systems in the literature are devoted to the frame-like structures representing multi-story buildings [17], hexagonal chiral lattices [18] or shell structures [19]. Available wave propagation studies of multi structural systems are mostly limited to the analysis of beams rigidly connected through periodically distributed ribs [20] or sandwich structures with a soft [21] or auxetic core [22]. In [21], the authors employed the asymptotic method to analyze a long-wave dynamic model of two layers adhesively connected by a thin and soft core. Particularly, they analyzed the propagation of waves along the thin interface layer and reviled some interesting effects such as coupling between the longitudinal and transverse displacements associated with a slow motion, and longitudinal displacement jumps related to fast motion. Similar problems has been addressed by other authors [23], where also asymptotic method was applied to study wave propagation in a three layer beam with a thin and soft core in the middle. In [24] the authors demonstrated that dynamics of two beams bonded by adhesive joint can be approximately represented by the Winkler and Pasternak type elastic layers for different boundary conditions. This paved the way for dynamic studies of sandwich beams [25], multi-beam [26] and multi-plate [27] systems coupled through discrete elastic or viscoelastic layers. If beam, plate or membrane structures are coupled, they are observed as layered systems having unique band structure properties [28,29] with a great potential for applications in wave absorption [30] and topological waveguiding [31].

According to [32], one can distinguish two main approaches to form the eigenvalue problem for wave propagation analysis in periodic structures.The first and the oldest is the inverse approach, where the propagation constant of a periodic structure is fixed while the unknown frequencies need to be computed. The second is the direct approach, which was later developed to avoid certain deficiencies of the inverse approach, but ill conditioning of the eigenvalue problem and possible low machine precision set limitations to this approach. Therefore, in [32] the authors proposed a combination of these two approaches when defining the eigenvalue problem. Different methods are used in the literature such as plane wave expansion [33], transfer matrix [34], finite element [35] or finite difference method [36], which all belong to the inverse approaches. In [37], the authors named the therein presented approach as the inverse method, where the band structure is determined without explicitly including the terms related to the material and geometrical properties except for the lattice constant, i.e. from the response of the system instead of using a model, as it is done in the majority of the methods available in the literature. Moreover, an interesting study [38] of elastic wave propagation in two-component laminates revealed the universal structure of its frequency spectrum independent of the geometry of the periodic-cell and the specific physical properties. In this study, an inverse Floquet-Bloch approach is applied to define the eigenvalue problem, where the corresponding inverse state-vector is formed after performing the discretization procedure.

The concept of locally resonant metamaterials is often used to form the periodic systems with low frequency bandgaps, in which the lattice dispersion characteristics depend on the modal behaviour of the host structure with its resonators [39]. Modal analysis was shown to be very useful in the nonlinear periodic structure analysis, were the Galerkin approximation method is applied to study the multi-mode vibration absorption capability of a nonlinear metamaterial Euler-Bernoulli beam coupled to a distributed array of nonlinear spring-mass subsystems behaving as local vibration absorbers [40]. Similar methodology was applied in [41], where frequencies of the attached resonators are tuned exactly to targeted modes of a non-

linear metamaterial beam. In [42], a general approach for estimation of the band structure of metamaterials with locally resonant properties is proposed. However, in [43] the authors demonstrated that the Bragg-type and resonance-type gaps can co-exist, which was explained through coupled bandgaps generated in the periodic system such as rod with multiple internal resonators. Since the first introduction of periodic materials with internal resonators [44], the mechanism responsible for the opening of locally resonant bandgaps has been investigated in a number of studies [45–47]. In [48] the authors identified the conditions for the transition between Bragg scattering and local resonance and showed the effects of this transition on the lowest bandgap. This was demonstrated on the examples of different types of materials, geometric and boundary periodicity in Timoshenko beams with and without elastically suspended masses. Moreover, another promissing application of metamaterials and periodic structures lies in seismic shielding over the entire range of frequencies. According to [49], three approaches are used to obtain shielding effects: Bragg scattering, locally resonant sub-wavelength inclusions and application of zero-frequency stop-band media. However, all three mechanisms for bandgap formation occur in a small number of periodic structures, thus providing the motivation for further investigations. Moreover, design of periodic structures is a powerful concept to achieve mechanical wave filtering. Different concepts for filtering of elastic waves are suggested in the literature. The concept based on structural interfaces, initially introduced in [50], involves a non-local mechanical behavior and allows the achievement of special mechanical properties. It was revealed in [51] that thick interfaces separating different regions of elastic materials introduce unique filtering characteristics that cannot be achieved with multilayered interfaces. In this paper, a unique band structure proprieties of the herein proposed systems reveal the presence of all three requirements needed for seismic shielding and wave filtering applications, such as the existence of zero-frequency and low-frequency bandgaps, as well as the bandgaps at higher dispersion branches.

The present paper shows the methodology for studying the wave propagation along the array of vertically aligned and elastically connected periodic structures (e.g. beams, plates, membranes or shallow shells) with the same boundary conditions and coupling medium stiffness. The main steps in defining the problem are the derivation of the system's governing equations, application of multi-mode Galerkin discretization and the assumption of wave propagation in the thickness direction of structural elements using the Floquet-Bloch theory. This methodology is generalized for one-dimensional case. Frequency band structure of the system is investigated by using the inverse approach to solve the eigenvalue problem and generate dispersion curves when the propagation constant is confined to the first Brillouin zone. The paper is organized as follows: the general mechanical model of periodic and coupled slender structures, Galerkin approximation procedure, Floquet-Bloch theorem and definition of the eigenvalue problem are presented in Section 2. The particular problem of wave propagation in an array of vertically aligned and elastically connected Rayleigh beams given in the so-called "diatomic" and "triatomic" unit cell configurations is detailed in Section 3. Section 4 shows the validation study of the methodology based on Galerkin approximation by using the finite element model, and the parametric study of the influence of coupling medium stiffness, concentrated masses and beam's boundary conditions on the frequency band structure of the proposed coupled beam-mass system.

2. Mathematical preliminaries

In order to analyze the free wave propagation in elastically connected structures such as beams, plates, strings or membranes, different approaches to discretize partial differential equations are used in the literature. The exact solutions of wave propagation problems in structural mechanics are difficult to find due to model complexities, such as specific boundary conditions, shape of structural elements, concentrated masses, attached vibration absorbers, etc. Therefore, application of approximate methods such as Rayleigh's, Rayleigh-Ritz or Galerkin approximation method can play an important role in solving the corresponding eigenvalue problems by approximating solutions using a finite number of mode shapes as admissible functions [52].

Here, we focus our attention to application of the Galerkin approximation in combination with Floquet-Bloch theorem to solve the corresponding eigenvalue problem. Typical unit cells of the proposed periodic system can be modelled as the diatomic and triatomic chains, composed of, respectively, two and three elastically connected structural elements such as beams or plates, Fig. 1.

2.1. The Galerkin approximation and inverse Floquet-Bloch formalism

The Galerkin approximation method belongs to a special group of weighted residual methods. The general solution of the problem is given as a linear combination of trial functions, which are chosen such that they exactly satisfy the corresponding boundary conditions.

Let us consider the m-th unit cell of an array of elastically connected slender structures, which is composed of several structural elements with each one having different material (density) or geometrical properties (thickness) than others. It is assumed that waves propagate only along the array of structural elements i.e. in the direction normal to the structures' length/surface, which is denoted by wavy line in Fig. 1. The general unit cell model of such systems is governed by the following equations of motion

$$\epsilon_i(x)\frac{\partial^2 w_i(x,t)}{\partial t^2} + \Pi_i[w_i(x,t)] + \Pi_{i+1}[w_{i+1}(x,t)] + \Pi_{i-1}[w_{i-1}(x,t)] = f_i(x,t), \quad i = 1,\ldots,p, \tag{1}$$

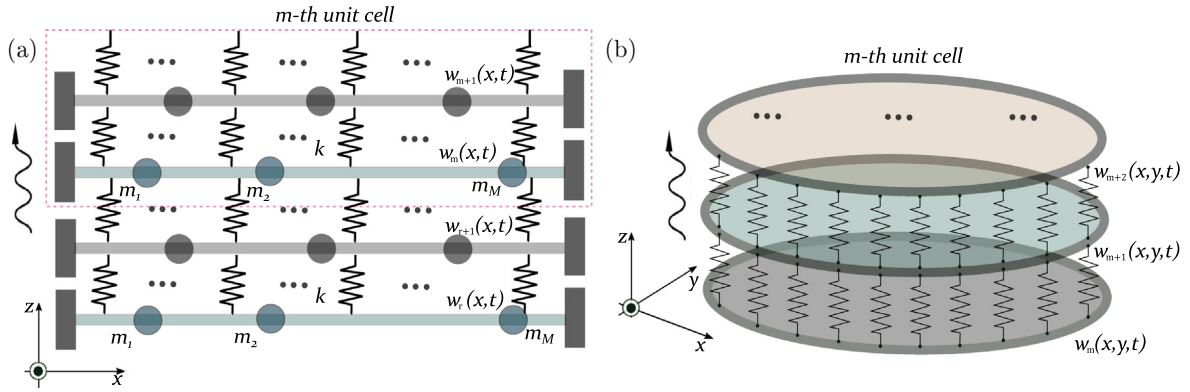

Fig. 1. The structural elastic models of unit cells proposed for: (a) a multi-beam-mass system formed as a diatomic unit cell and (b) a multi-plate system modelled as a triatomic unit cell. The wavy line shows the direction of the wave propagation through the periodic slender structures.

where p denotes the number of structures in a chosen unit cell, $\epsilon_i(x)$ is the inertia term of the considered element and $f_i(x,t)$ is the external excitation. When $p=2$ the system is named diatomic chain and for $p=3$ it is called triatomic chain [53]. The masses of the beams within a cell differ due to different geometrical and material properties or a different number of attached concentrated masses. Assuming the solution of $w_i(x,t)$ in the form of a series of N comparison functions and time generalized coordinates yields

$$w_i(x,t)=\sum_{k=1}^{N} q_{(i)k}(t)\phi_k(x)=\mathbf{C}\mathbf{q}_i, \quad i=1,\ldots,p, \tag{2}$$

in which $\mathbf{q}_i=[q_{(i)1}(t),q_{(i)2}(t),\ldots,q_{(i)N}(t)]^T$ represents the vector of time functions of the i-th structural element and $\mathbf{C}=[\phi_1(x),\phi_2(x),\ldots,\phi_N(x)]$ is the vector of the assumed mode shapes that satisfy the geometric and natural boundary conditions, and which are differentiable at least up to the highest order of spacial derivative in the differential equation of motion Eq. (1). The same boundary conditions are applied to all structural elements in the system. In general, the approximated solution Eq. (2) satisfies all boundary conditions of the unit cell except for the equations of motion Eq. (1). By introducing Eq. (2) into the differential equation of motion Eq. (1), the resulting equation will define the i-th residue as

$$\ell_i(x,t) := \epsilon_i(x)\mathbf{C}\ddot{\mathbf{q}}_i+\Pi_i[\mathbf{C}]\mathbf{q}_i+\Pi_{i+1}[\mathbf{C}]\mathbf{q}_{i+1}+\Pi_{i-1}[\mathbf{C}]\mathbf{q}_{i-1}-f_i(x,t)=0, \quad i=1,\ldots,p, \tag{3}$$

where $\Pi_i[\mathbf{C}]=(\Pi_i[\phi_1(x)],\Pi_i[\phi_2(x)],\ldots,\Pi_i[\phi_N(x)])$. It should be noted that all the residuals will be equal to zero because trial solution is composed of comparison functions that satisfy all the boundary conditions. According to the criteria of the Galerkin method, all residuals should be small. In other words, residue should have zero projection on the chosen basis functions $\phi_j(x)$, $j=1,\ldots,N$ since approximated solution is placed in finite N-dimensional space. For the case of m unit cells, which depends on the number of structural components, the solution will be extended to a number p. Therefore, multiplying the i-th residual by comparison functions and then integrating their product over the domain of a specific structural components gives

$$<\ell_i(x,t),\phi_j(x)> := \int_0^l \ell_i(x,t)\phi_j(x)dx=0, \quad j=1,\ldots,N, \quad i=1,\ldots,p. \tag{4}$$

Introducing the expression Eq. (3) into Eq. (4) and after integration, the set of ordinary differential equation appears with the corresponding mass and stiffness matrices in the following form

$$\mathbf{M}_i\ddot{\mathbf{q}}_i+\mathbf{K}_i\mathbf{q}_i+\mathbf{K}_{i+1}\mathbf{q}_{i+1}+\mathbf{K}_{i-1}\mathbf{q}_{i-1}=\mathbf{f}_i, \quad i=1,\ldots,p, \tag{5}$$

where the elements of the mass and stiffness matrices and the force vector are determined as

$$\begin{aligned}&\mathbf{M}_i=\textstyle\int_0^l \epsilon_i(x)\mathbf{C}^T\mathbf{C}dx, \quad \mathbf{K}_i=\int_0^l \mathbf{C}^T\Pi_i[\mathbf{C}]dx, \quad i=1,\ldots,p,\\ &\mathbf{K}_{i+1}=\textstyle\int_0^l \mathbf{C}^T\Pi_{i+1}[\mathbf{C}]dx, \quad \mathbf{K}_{i-1}=\int_0^l \mathbf{C}^T\Pi_{i-1}[\mathbf{C}]dx, \quad \mathbf{f}_i=\int_0^l \mathbf{C}^T f_i dx.\end{aligned} \tag{6}$$

In general, for the m-th unit cell composed of p structural elements it holds

$$\mathbf{M}_m\ddot{\mathbf{q}}_m(t)+\mathbf{K}_m\mathbf{q}_m(t)+\mathbf{K}_{m+1}\mathbf{q}_{m+1}(t)+\mathbf{K}_{m-1}\mathbf{q}_{m-1}(t)=\mathbf{F}_m, \tag{7}$$

where the mass and stiffness matrices of the unit cell are given in Appendix A. The generalized time coordinates are given as $\mathbf{q}_m=[q_{(1)1}(t),\ldots,q_{(1)N}(t),\ldots,q_{(p)1}(t)\ldots,q_{(p)N}(t)]^T$. To analyze the wave propagation, the harmonic solution is assumed by neglecting the vector of external forces. Assuming that $\mathbf{q}_m(t)=\bar{\mathbf{q}}_m e^{j\omega t}$ and introducing it in Eq. (7), yields

$$(\mathbf{K}_m - \omega^2\mathbf{M}_m)\bar{\mathbf{q}}_m + \mathbf{K}_{m+1}\bar{\mathbf{q}}_{m+1} + \mathbf{K}_{m-1}\bar{\mathbf{q}}_{m-1} = \mathbf{0}. \tag{8}$$

It is also assumed that unit cells are repeating periodically in the thickness direction i.e. normal to the length/surface of the structural elements. Note that a unit cell and its neighbors in Eq. (8) may be identified by $\mathbf{K}_m = \mathbf{K}_u$, where $\mathbf{K}_u$ with $u = -1, 0, 1$ denotes the previous, present and subsequent unit cell, respectively as given in [29].

For determination of dispersion characteristics of the system, the inverse method is introduced as given in [29,37]. The dispersion curves are given by the wave frequency ω as a function of propagation constant μ. By considering the undamped Bloch wave propagation, the corresponding eigenvalue problem can be formulated by using the expression given in Eq. (8). However, only the real part of the dispersion curve without attenuation is observed.

To obtain the frequency band structure, i.e. dispersion diagrams, the solution procedure based on the Floquet-Bloch theorem [29] is applied to Eq. (8). The assumed plane wave solution is defined as

$$\bar{\mathbf{q}}_m(\omega) = \tilde{\mathbf{q}}(\mu)e^{jm\mu}, \tag{9}$$

in which the value of the propagation constant μ is pre-set. Inserting the assumed plane wave solution Eq. (9) into Eq. (8) yields the following linear eigenvalue problem

$$(\mathbf{K} - \omega^2\mathbf{M})\tilde{\mathbf{q}}(\mu)e^{jm\mu} = \mathbf{0}, \tag{10}$$

where the overall stiffness matrix is derived as

$$\mathbf{K} = \mathbf{K}_{-1}e^{-j\mu} + \mathbf{K}_0 + \mathbf{K}_{+1}e^{+j\mu} = \sum_{u=-1,0,1}(\mathbf{K}_u e^{ju\mu}). \tag{11}$$

The solution of the eigenvalue problem for the m-th unit cell obtained in Eq. (10) gives corresponding dispersion diagrams. Solution of this problem requires the propagation constant μ to be known, which is taken within the First Brillouin Zone (FBZ) fundamental period of the dispersion relation, determined for one-dimensional periodic structures in the range $-\pi \leqslant \mu \leqslant \pi$, [53]. As stated in [29], for the wave propagation in periodic structures without attenuation, the wave propagation constant μ corresponds to a real value. On the other hand, the imaginary values of the propagation constant μ are related to the spatial decay of the wave amplitude as the wave propagates through a periodic structure. The number of dispersion curves resulting from the solution of the eigenvalue problem directly depends on the number of connected structural elements (p) in the unit cell and the number of considered terms in the Galerkin approximation (N). The band structure defines the position and width of pass and stop bands (bandgaps). It is well known that the pass-bands are related to the frequency ranges where an elastic wave propagates through the periodic structure, while bandgaps are frequency ranges where waves are attenuated.

3. Problem formulation

3.1. Motion equations of an array of elastically connected beams

In this section, an example of a periodic structure based on elastically coupled beams with concentrated masses is presented to demonstrate the efficiency of the approach based on the Galerkin approximation and Floquet-Bloch theorem. It is well known that classical Euler-Bernoulli beam theory is often used for accurate modelling of long and slender beams, whereas to accurately predict frequencies at higher modes of thick and short beams one should use higher order theories such as Timoshenko's beam theory. Lord Rayleigh developed simpler theory that includes the rotary inertia effect but without the complexity of the Timoshenko's beam theory. Nevertheless, Rayleigh's beam theory can predict response of slender beam structures with a satisfying accuracy.

Introducing the heterogeneity in the system is a major requirement to obtain the wave dispersion properties, which is achieved by taking into account diatomic and triatomic unit cell configurations with two and three elastically connected beams, respectively, having different material or geometrical properties such as density or beam's height. It is assumed that unit cells are periodically distributed in z- direction to infinity, as shown in Fig. 2. Moreover, identical boundary conditions are assumed for all beams within the system (unit cells), which are mutually connected through the continuously distributed springs i.e. Winkler's type of elastic medium. In this analysis, two types of beam's boundary conditions were considered: clamped-free (Fig. 2(a)) and simply supported (Fig. 2(b)).

By introducing the assumptions from the Rayleigh's beam theory [13,52], the governing equation of motion for the infinite periodic system, with p structural elements in the unit cell, can be derived by using the Hamilton's principle as

$$\begin{aligned} &E_{si}I_{si}\frac{\partial^4 w_{si}}{\partial x^4} + k(w_{si} - w_{(s-1)(i-1)}) + k(w_{si} - w_{(s+1)(i+1)}) - \rho_{si}I_{si}\frac{\partial^4 w_{si}}{\partial t^2 \partial x^2} \\ &\quad + \left[\rho_{si}A_{si} + \sum_{b=1}^{M_{si}} M_{b(si)}\delta(x - a_{b(si)})\right]\frac{\partial^2 w_{si}}{\partial t^2} = f_{si}(x,t), \end{aligned} \tag{12}$$

where $w_{si} = w_{si}(x,t)$ and $f_{si} = f_{si}(x,t)$ are the transverse displacement and external load, respectively of the s-th beam in the multiple beam system, and i-th beam in the unit cell, while k is the stiffness of Winkler's elastic medium. The indices i and s

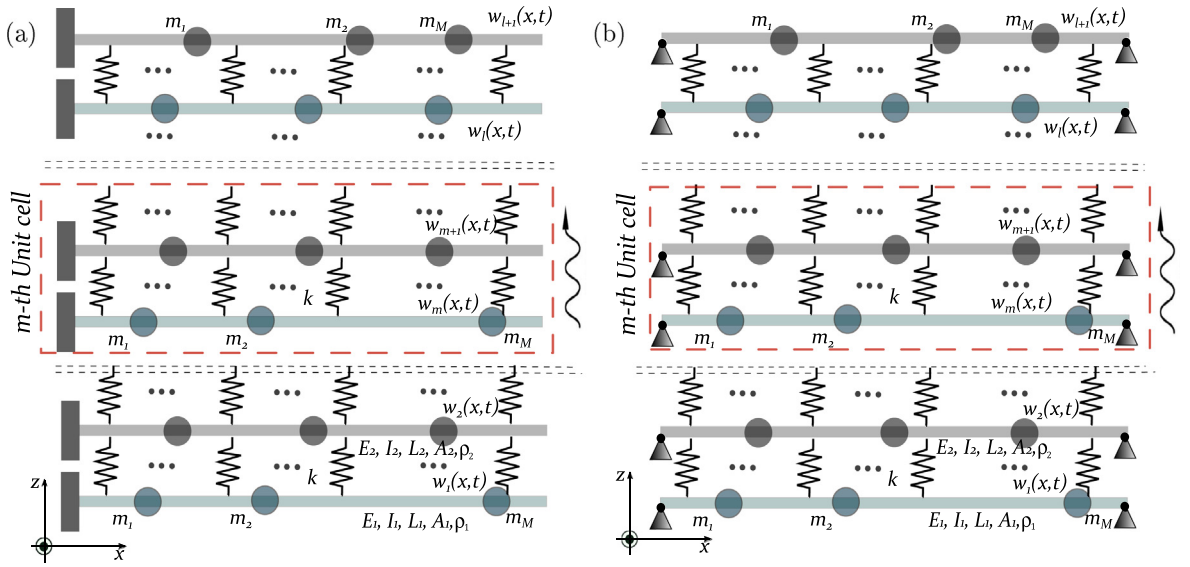

Fig. 2. Periodic system of elastically connected Rayleigh beams with concentrated masses (a) the clamped-free and (b) the simply-supported boundary conditions. The unit cell composed of two elastically connected Rayleigh beams is named diatomic cell.

can take the following values, $s = 1, 2, 3 \ldots$and $i = 1, 2, \ldots, p$, where p is the number of beams in the unit cell. The material and geometrical characteristics of the si-th beam are given by Young's modulus E_{si} , mass density ρ_{si}, cross-sectional area A_{si} and moment of inertia I_{si}. The term $M_{b(si)}$ denotes the b-th attached point mass on the position $a_{b(si)}$ in the axial direction of each beam in the system.

The adopted boundary conditions for clamped-free (CF) and simply-supported (SS) beams are given as

$$w_{si}(0,t) = \frac{\partial w_{si}(0,t)}{\partial x} = \frac{\partial^2 w_{si}(L,t)}{\partial x^2} = \frac{\partial^3 w_{si}(L,t)}{\partial x^3} = 0, \tag{13}$$

and

$$w_{si}(0,t) = \frac{\partial^2 w_{si}(0,t)}{\partial x^2} = w_{si}(L,t) = \frac{\partial^2 w_{si}(L,t)}{\partial x^2} = 0. \tag{14}$$

The initial conditions are taken to be zero.

Taking into consideration the m-th unit cell of the periodic structure modeled as diatomic $p = 2$ and triatomic $p = 3$ system, the governing equations can be reduced to

diatomic unit cell:

$$E_1 I_1 \frac{\partial^4 w_m}{\partial x^4} + k(w_m - w_{m-1}) + k(w_m - w_{m+1}) \tag{15}$$

$$+ \left[\rho_1 A_1 + \sum_{b=1}^{M_1} M_{b(1)} \delta(x - a_{b(1)})\right] \frac{\partial^2 w_m}{\partial t^2} - \rho_1 I_1 \frac{\partial^4 w_m}{\partial t^2 \partial x^2} = f_m(x,t),$$

$$E_2 I_2 \frac{\partial^4 w_{m+1}}{\partial x^4} + k(w_{m+1} - w_m) + k(w_{m+1} - w_{m+2}) \tag{16}$$

$$+ \left[\rho_2 A_2 + \sum_{b=1}^{M_2} M_{b(2)} \delta(x - a_{b(2)})\right] \frac{\partial^2 w_{m+1}}{\partial t^2} - \rho_2 I_2 \frac{\partial^4 w_{m+1}}{\partial t^2 \partial x^2} = f_{m+1}(x,t),$$

triatomic unit cell:

$$E_1 I_1 \frac{\partial^4 w_m}{\partial x^4} + k(w_m - w_{m-1}) + k(w_m - w_{m+1}) \tag{17}$$

$$+ \left[\rho_1 A_1 + \sum_{b=1}^{M_1} M_{b(1)} \delta(x - a_{b(1)})\right] \frac{\partial^2 w_m}{\partial t^2} - \rho_1 I_1 \frac{\partial^4 w_m}{\partial t^2 \partial x^2} = f_m(x,t),$$

$$E_2I_2\frac{\partial^4 w_{m+1}}{\partial x^4}+k(w_{m+1}-w_m)+k(w_{m+1}-w_{m+2})+ \tag{18}$$
$$\left[\rho_2A_2+\sum_{p=1}^{M_2}M_{b(2)}\delta(x-a_{b(2)})\right]\frac{\partial^2 w_{m+1}}{\partial t^2}-\rho_2I_2\frac{\partial^4 w_{m+1}}{\partial t^2\partial x^2}=f_{m+1}(x,t),$$

$$E_3I_3\frac{\partial^4 w_{m+2}}{\partial x^4}+k(w_{m+2}-w_{m+1})+k(w_{m+2}-w_{m+3})+ \tag{19}$$
$$\left[\rho_3A_3+\sum_{p=1}^{M_3}M_{b(3)}\delta(x-a_{b(3)})\right]\frac{\partial^2 w_{m+2}}{\partial t^2}-\rho_3I_3\frac{\partial^4 w_{m+2}}{\partial t^2\partial x^2}=f_{m+2}(x,t).$$

3.2. Defining the eigenvalue problem

In order to analyse the free wave propagation through the periodic structure, the approach based on the Galerkin discretization and Floquet-Bloch theorem is applied for the chosen unit cell defined in the previous section. The main objective is to determine the band structures by detecting stop and pass bands in order to demonstrate the applicability of the presented methodology. In the following, derivations are given for the diatomic chain system, which can be easily extended to the triatomic case.

The first step is to discretize the motion equations of the unit cell by using the Galerkin approximation, which for the $i-th$ beam in the $m-th$ unit cell is defined as

$$w_i(x,t)=\sum_{k=1}^{N}q_{(i)k}(t)\phi_k(x),\quad i=1,\dots,p, \tag{20}$$

where $q_{(i)k}(t)$ and $\phi_k(x)$ are the $k-th$ generalized time function and assumed trial (mode shape) function of the $i-th$ beam. N is the number of terms in the Galerkin approximation series. Inserting Eq. (20) into the equations for unit cell Eq. (15)–(19) yields

$$\begin{aligned}&\sum_{k=1}^{N}E_iI_iq_{(i)k}\phi_k''''+\sum_{k=1}^{N}2kq_{(i)k}\phi_k+\sum_{k=1}^{N}\left[\rho_iA_i+\sum_{b=1}^{M_i}M_{b(i)}\delta(x-a_{b(i)})\right]\ddot{q}_{(i)k}\phi_k-\\&-\sum_{k=1}^{N}\rho_iI_i\ddot{q}_{(i)k}\phi_k''-\sum_{k=1}^{N}kq_{(i-1)k}\phi_k-\sum_{k=1}^{N}kq_{(i+1)k}\phi_k-f_i(x,t)=\ell_i(x,t),\quad i=1,\dots,p,\end{aligned} \tag{21}$$

where ℓ_i is the $i-th$ non-zero residue obtained from the introduced approximated solution. By multiplying the above expression with the $j-th$ trial function ϕ_j for $j=1,2,\dots,N$ and integrating over the beam's length, the following system of equations is obtained

$$\begin{aligned}&\sum_{k=1}^{N}E_iI_i\left(\int_0^L\phi_k''''\phi_j dx\right)q_{(i)k}+\sum_{k=1}^{N}2k\left(\int_0^L\phi_k\phi_j dx\right)q_{(i)k}+\\&+\sum_{k=1}^{N}\left(\int_0^L\left[\rho_iA_i+\sum_{b=1}^{M_i}M_{b(i)}\delta(x-a_{b(i)})\right]\phi_k\phi_j dx\right)\ddot{q}_{(i)k}-\\&-\sum_{k=1}^{N}\rho_iI_i\left(\int_0^L\phi_k''\phi_j dx\right)\ddot{q}_{(i)k}-\sum_{k=1}^{N}k\left(\int_0^L\phi_k\phi_j dx\right)q_{(i-1)k}-\\&-\sum_{k=1}^{N}k\left(\int_0^L\phi_k\phi_j dx\right)q_{(i+1)k}=\left(\int_0^Lf_i(x,t)\phi_j dx\right),\quad i=1,\dots,p.\end{aligned} \tag{22}$$

or in a more compact form as

$$\sum_{k=1}^{N}M_{jk}^{(i)}\ddot{q}_{(i)k}+\sum_{k=1}^{N}K_{jk}^{(i)}q_{(i)k}+\sum_{k=1}^{N}B_{jk}^{(i)}q_{(i+1)k}+\sum_{k=1}^{N}B_{jk}^{(i)}q_{(i-1)k}=F_j^{(i)},\quad i=1,\dots,p., \tag{23}$$

where

$$\begin{aligned}M_{jk}^{(i)}&=\left(\int_0^L\left[\rho_iA_i+\sum_{b=1}^{M_i}M_{b(i)}\delta(x-a_{b(i)})\right]\phi_k\phi_j dx\right)-\rho_iI_i\left(\int_0^L\phi_k''\phi_j dx\right),\\K_{jk}^{(i)}&=E_iI_i\left(\int_0^L\phi_k''''\phi_j dx\right)+2k\left(\int_0^L\phi_k\phi_j dx\right),\\B_{jk}^{(i)}&=-k\left(\int_0^L\phi_k\phi_j dx\right),\quad F_j^{(i)}=\int_0^Lf_i(x,t)\phi_j dx,\quad i=1,\dots,p.\end{aligned} \tag{24}$$

To apply the solution based on the Floquet-Bloch's theorem, the expression given in Eq. (23) should be rewritten in the matrix form that is more convenient for the following analysis. By assuming a harmonic solution for the generalized time functions and neglecting the external load, the system of Eqs. Eq. (23) for $m-th$ unit cell takes a new form

$$\mathbf{D}_m(\omega)\tilde{\mathbf{q}}_m + \mathbf{K}_{m+1}\tilde{\mathbf{q}}_{m+1} + \mathbf{K}_{m-1}\tilde{\mathbf{q}}_{m-1} = \mathbf{0}, \tag{25}$$

where $\mathbf{D}_m(\omega)$ is related to the dynamic stiffness matrix of the unit cell, and matrices $\mathbf{K}_{m+1}$ and $\mathbf{K}_{m-1}$ denote additional stiffness defined for the triatomic chain model as

$$\mathbf{D}_m(\omega) = \left(\begin{bmatrix} \mathbf{K}_1 & \mathbf{0} & \mathbf{0} \\ \mathbf{0} & \mathbf{K}_2 & \mathbf{0} \\ \mathbf{0} & \mathbf{0} & \mathbf{K}_3 \end{bmatrix} - \omega^2 \begin{bmatrix} \mathbf{M}_1 & \mathbf{0} & \mathbf{0} \\ \mathbf{0} & \mathbf{M}_2 & \mathbf{0} \\ \mathbf{0} & \mathbf{0} & \mathbf{M}_3 \end{bmatrix} \right), \tag{26}$$

$$\mathbf{K}_{m+1} = \mathbf{K}_{m-1} = \begin{bmatrix} \mathbf{B}_1 & \mathbf{0} & \mathbf{0} \\ \mathbf{0} & \mathbf{B}_2 & \mathbf{0} \\ \mathbf{0} & \mathbf{0} & \mathbf{B}_3 \end{bmatrix},$$

and the vectors of generalized coordinates are

$$\tilde{\mathbf{q}}_m = \begin{bmatrix} \mathbf{q}_m \\ \mathbf{q}_{m+1} \\ \mathbf{q}_{m+2} \end{bmatrix}, \tilde{\mathbf{q}}_{m-1} = \begin{bmatrix} \mathbf{q}_{m-1} \\ \mathbf{q}_m \\ \mathbf{q}_{m+1} \end{bmatrix}, \tilde{\mathbf{q}}_{m+1} = \begin{bmatrix} \mathbf{q}_{m+1} \\ \mathbf{q}_{m+2} \\ \mathbf{q}_{m+3} \end{bmatrix}. \tag{27}$$

By inserting the solution Eq. (9) into the Eq. (25), the following eigenvalue problem is obtained

$$\tilde{\mathbf{D}}(\omega)\tilde{\mathbf{q}}(\mu)e^{jm\mu} = \mathbf{0}, \tag{28}$$

where the dynamic stiffness matrix is derived as

$$\tilde{\mathbf{D}}(\omega) = \tilde{\mathbf{K}}_{-1}e^{-j\mu} + \tilde{\mathbf{K}}_0 + \tilde{\mathbf{K}}_{+1}e^{+j\mu} - \omega^2\tilde{\mathbf{M}}. \tag{29}$$

Solving the eigenvalue problem Eq. (28) for given values of propagation constant μ, one can obtain the corresponding dispersion curves of the system. It can be noticed that the obtained eigenvalue problems are similar to the ones derived for equivalent discrete models of diatomic and triatomic phononic crystals, having two and three different masses within the unit cell, respectively. Similar conclusions are brought in [31], where topological pumping was studied in a similar system of elastically coupled beams. In this study the main focus is put on the investigation of wave propagation in a heterogeneous systems of elastically connected beams with unit cell configurations having two and three beams of different geometrical or material properties.

4. Numerical study

In this section, the frequency band structures of a periodic system based on multiple elastically connected Raleigh beams with concentrated masses is investigated by using the methodology elaborated in Section 3. Two different unit cell configurations, such as diatomic and triatomic chain systems, are adopted in the numerical study. The results obtained by the Galerkin approximation and Floquet-Bloch theory are validated against the results from the finite element model and those obtained by the frequency response function (FRF). The effects of coupling medium stiffness k and concentrated masses M_p on the band structure of the system are examined in detail. Additionally, the influence of boundary conditions, number of adopted terms in the Galerkin approximation and different unit cell configurations are studied and discussed. To achieve the desired wave dispersion properties, the heterogeneity of the system is introduced by assuming beams in the unit cell with different material or geometrical properties. Numerical simulations are performed for $N = 5$ terms in the Galerkin approximation. Moreover, in validation study, the finite element (FE) method is used to determine the frequency band structure and to compare the results obtained by the Galerkin approximation, where fine agreement is achieved. More details on FE models of multiple beam systems can be found in [54,26]. In the presented study every beam in the unit cell is approximated by considering $n_{ele} = 50$ Rayleigh beam elements.

4.1. Validation

The presented FRF solution is obtained by taking the same number of terms in the Galerkin approximation as in the Floquet-Bloch analysis, and a finite number of unit cells. The following material and geometrical parameters are used in simulations if not specified differently: the cross-sectional area $A = bh$ and the second moment of inertia $I = \frac{bh^3}{12}$for the first beam in the unit cell with height $h = 0.003(\mathrm{m})$ and width $b = 0.02(\mathrm{m})$. Length of all beams in the system is adopted as $L = 0.8(\mathrm{m})$, while mass density of the first beam is given as $\rho = 1190.0(\mathrm{kg/m^3})$, elastic modulus as $E = 3.2 \cdot 10^9(\mathrm{Pa})$ and the number of concentrated masses per beam as $M = 3$, each weighting one third of beam's weight. The positions of attached point masses

are identical for each beam in the system, where $a_b = (\frac{1}{3}, \frac{1}{2}, \frac{2}{3})L$. In order to analyse the harmonic response using FRF, the system with ten connected unit cells is observed. The harmonic force is applied at the middle of the first beam for the simply supported boundary conditions and at the free end of the beam for the clamped-free case. The response is measured at the last beam in the periodic system, where the first beam is those where the coordinate system is placed. The stiffness of the coupling Winkler's type elastic medium is adopted as $k = 100(\mathrm{N/m^2})$. Moreover, Table 1 shows properties of beam elements within the unit cell of a periodic structure in four different configurations with simply supported (SS) and clamped-free (CF) boundary conditions for diatomic and triatomic unit cell configurations. Here, all calculations are given for the normalized frequency given as $\Omega = \omega/\omega_0$, where $\omega_0 = \frac{\pi^2}{L^2}\sqrt{\frac{E_1 I_1}{\rho_1 A_1}}$ is the first natural frequency of the simply-supported beam. Fig. 3 shows comparison of the band structures of systems with elastically connected beams and attached concentrated masses, given in the diatomic and triatomic unit cell configurations, against FRF results of the equivalent system with a finite number of unit cells. Simulations are performed for the five considered terms in the Galerkin approximation and mode shapes of simply supported beams adopted as admissible functions. One can notice similar stop-bands (colored in yellow) and transmission-bands in both the dispersion and FRF diagrams. One can be observe five bandgaps starting from narrower and lower frequency bandgaps and than going to wider and higher frequency bandgaps. In the case of the triatomic configuration given in Fig. 3 b), a higher number of bandgaps can be identified. Here, eight bandgaps can be noticed in the given frequency range in both the dispersion and FRF diagrams. Similar to the previous case, the narrowest bandgap is located at lower frequency dispersion curves while the others are slightly wider. Moreover, in both configurations one can notice a very narrow bandgap at the lowest possible frequency usually named zero-frequency bandgap, whose appearance can be attributed to the presence of the coupling Winkler type of elastic medium [12] or boundary conditions [49]. Additional validation is performed by comparing the dispersion curves obtained via Galerkin approximation and those obtained via the FE model and Floquet-Bloch solution that are marked as red circles in the figures. Comparison of the obtained dispersion characteristics using these two approaches shows excellent agreement of the results.

In Fig. 4, dispersion curves are given for the diatomic and triatomic unit cell configurations of the periodic system of elastically connected beams with five terms in the Galerkin approximation and mode shapes of clamped-free beams adopted as trial functions. One can observe several stop and transmission bands in both diatomic and triatomic configurations and good correspondence between the dispersion curves and FRF responses. It is obvious that lower frequency bandgaps are narrower than those at higher frequency ranges. In the clamped-free case the lower bandgap is shifted to higher frequency than in the simply supported case. The comparison of the Galerkin approximation results with the results from the FE model shows good agreement. The validation demonstrated the applicability, accuracy and simplicity of the proposed approach in analysing the band structure of the complex periodic system of elastically connected Rayleigh beams with concentrated masses that will be used in the following parametric study. Moreover, one can also notice that the introduction of the clamped-free boundary conditions on beams reduces the width of the initial zero-frequency bandgap.

4.2. Parametric study and discussion

The effects of beams' material/geometrical properties and boundary conditions

The effects of different geometrical properties as well as boundary conditions of beams in the unit cell of the proposed periodic system are investigated to reveal their influence on the frequency band structure. To see these effects, first periodic

Table 1
The values of parameters used in simulations of diatomic and triatomic unit cell configurations, whit results plotted in Figs. 3 and 4.

SS boundary conditions				
diatomic UC		triatomic UC		
Beam 1	Beam 2	Beam 1	Beam 2	Beam 3
$E_1 = E$	$E_2 = E$	$E_1 = E$	$E_2 = 2E$	$E_3 = 3E$
$\rho_1 = \rho$	$\rho_2 = \rho$	$\rho_1 = \rho$	$\rho_2 = \rho$	$\rho_3 = \rho$
$I_1 = \frac{bh^3}{12}$	$I_2 = \frac{b(2h)^3}{12}$	$I_1 = \frac{bh^3}{12}$	$I_2 = \frac{b(2h)^3}{12}$	$I_3 = \frac{bh^3}{12}$
$A_1 = bh$	$A_2 = 2bh$	$A_1 = bh$	$A_2 = 2bh$	$A_3 = bh$
$M_b = \frac{1}{3}\rho AL$	$M_b = \frac{1}{3}\rho AL$	$M_b = \frac{1}{2}\rho AL$	$M_b = \frac{1}{2}\rho AL$	$M_b = \frac{1}{2}\rho AL$
CF boundary conditions				
diatomic UC		triatomic UC		
Beam 1	Beam 2	Beam 1	Beam 2	Beam 3
$E_1 = E$	$E_2 = 3E$	$E_1 = E$	$E_2 = 2E$	$E_3 = 3E$
$\rho_1 = \rho$	$\rho_2 = \rho$	$\rho_1 = \rho$	$\rho_2 = \rho$	$\rho_3 = 1.5\rho$
$I_1 = \frac{bh^3}{12}$	$I_2 = \frac{b(2h)^3}{12}$	$I_1 = \frac{bh^3}{12}$	$I_2 = \frac{b(2h)^3}{12}$	$I_3 = \frac{bh^3}{12}$
$A_1 = bh$	$A_2 = 2bh$	$A_1 = bh$	$A_2 = 2bh$	$A_3 = bh$
$M_b = \frac{1}{3}\rho AL$	$M_b = \frac{1}{3}\rho AL$	$M_b = \frac{1}{2}\rho AL$	$M_b = \frac{1}{2}\rho AL$	$M_b = \frac{1}{2}\rho AL$

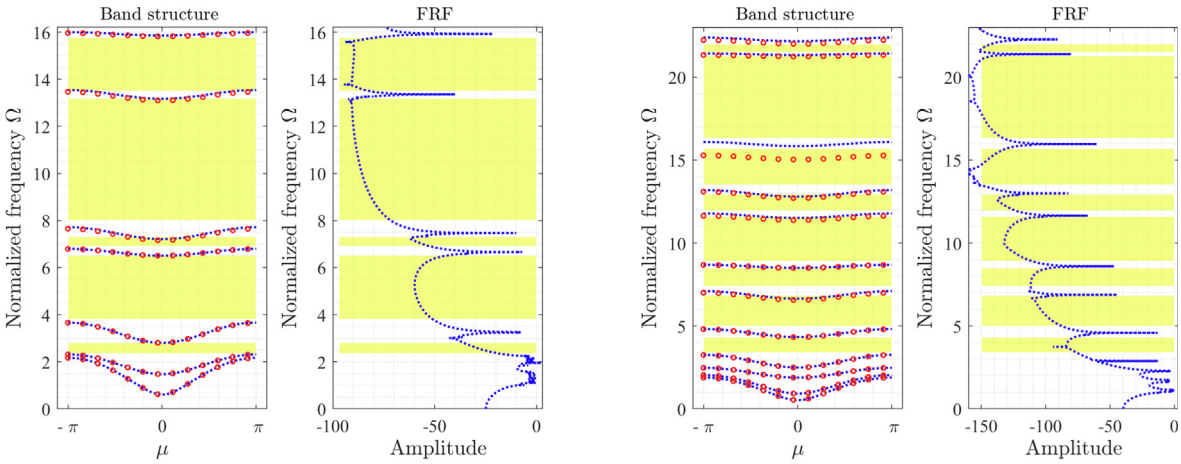

(a) The diatomic unit cell model. (b) The triatomic unit cell model.

Fig. 3. The frequency band structure of the diatomic and triatomic unit cell configurations of the periodic system of elastically connected Rayleigh beams with simply supported boundary conditions and FRF diagrams of the equivalent periodic system with ten unit cells. Blue doted lines are dispersion curves for the five terms in Galerkin approximation and red circles are results from the finite element model. (For interpretation of the references to color in this figure legend, the reader is referred to the web version of this article.)

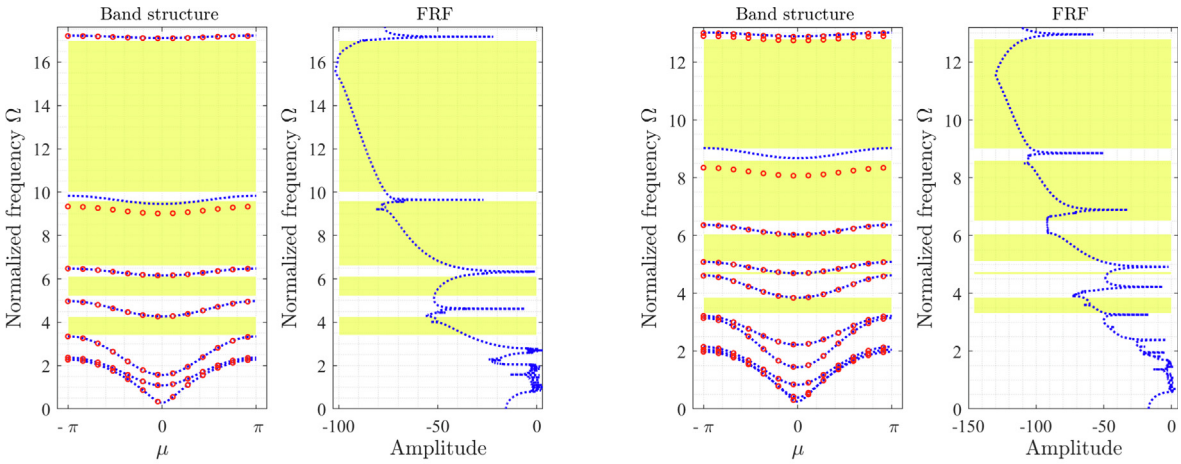

(a) The diatomic unit cell model. (b) The triatomic unit cell model.

Fig. 4. The frequency band structure of the diatomic and triatomic unit cell configurations of the periodic system of elastically connected Rayleigh beams with clamped-free boundary conditions and FRF diagrams of the equivalent periodic system with ten unit cells. Blue doted lines are dispersion curves for the five terms in Galerkin approximation and red circles are results from the finite element model. (For interpretation of the references to color in this figure legend, the reader is referred to the web version of this article.)

systems with diatomic and triatomic unit cell configurations are considered having two and three elastically connected identical beams, respectively for simply-supported and clamped-free boundary conditions, Fig. 5. Here, the same values of parameters as in the validation study are adopted except all the beams have the same cross sectional area, thus, having the same material and geometrical characteristics. The number of adopted terms in the Galerkin approximation is $N = 5$. It can be observed that there are four bandgaps plus the zero-frequency bandgap for the simply-supported boundary conditions case and only three bandgaps in the clamped-free boundary condition case. The reason for the lower number of visible dispersion curves is related to their overlapping due to identical beams in the unit cell having the same eigenfrequency properties. This means that the proposed system with identical unit cells can be represented by a monoatomic unit cell configuration with a single beam, which will generate the same band structure similar to discrete monoatomic chains. Lower bandgaps are narrower compared to the one at higher frequency, whereas the lowest bandgap in the clamped-free case is shifted to higher frequency compared to the simply supported case. In general, the case with identical beams exhibits a great wave attenuation potential since wide bandgaps are achieved with a minimal number of transmission-bands in between.

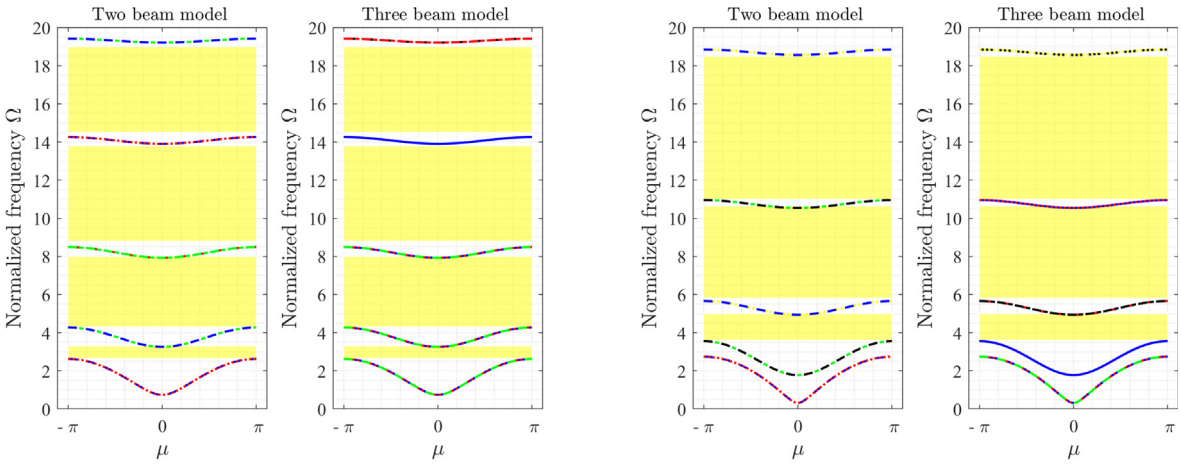

(a) The simply-supported boundary conditions. (b) The clamped-free boundary conditions.

Fig. 5. The frequency band structure of a periodic system with elastically connected beams and concentrated masses determined for five terms considered in Galerkin approximation. The unit cell configurations are based on coupled two and three identical beams, for two types of boundary conditions (a) simply-supported and (b) clamped-free.

The next figure shows the effects of different geometrical (cross sectional area) properties and boundary conditions of beams within the diatomic and tri atomic unit cell configurations on the frequency band structure diagrams. Fig. 6(a) shows eight regular bandgaps and one very narrow zero-frequency bandgap in the diatomic unit cell configuration and nine regular and one narrow zero-frequency bandgap in the triatomic case. The main difference between these two cases is in the number of dispersion curves witch is greater for the triatomic case due to the additional beam introduced in the unit cell. Fig. 6(b) shows the same unit cell models but for the clamped-free boundary conditions. It can be noticed that five bandgaps are obtained in the diatomic configuration and six for the triatomic case. However, additional zero-frequency band gaps in both cases are very narrow, almost invisible. Except for the additional bandgap at highest frequency there is no significant difference in width between other bandgaps. The first bandgap at the lowest frequency is the narrowest, which could be attributed to the local resonance nature of certain bandgaps. Generally, the effect of clamped-free boundary conditions is reflected in the vanishing of one bandgap at lower frequencies and the narrowing of other bandgaps. Different cross sectional areas of beams in Fig. 6 results in their different eifenfrequency properties and consequently in different dispersion characteristics. In this case, there is no overlapping of curves and higher number of dispersion branches can be detected compared to the case with identical beams for the same frequency range.

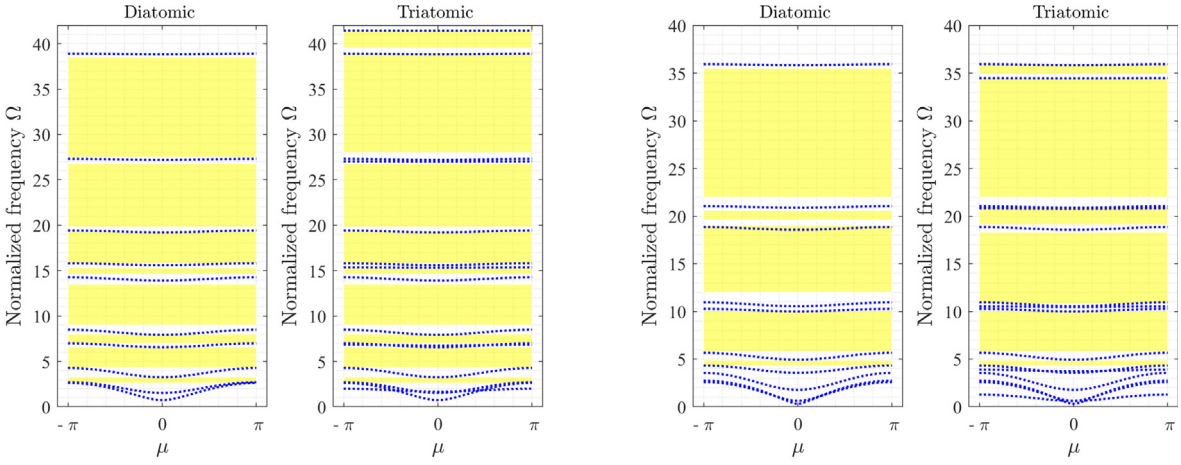

(a) The simply-supported boundary conditions. (b) The clamped-free boundary conditions.

Fig. 6. The frequency band structure of a periodic system with elastically connected beams and concentrated masses determined for five terms considered in the Galerkin approximation. The diatomic and triatomic unit cell configurations are based on coupled two and three beams with different geometrical properties, and for two types of boundary conditions (a) simply-supported and (b) clamped-free.

4.3. The effect of the stiffness of Winkler's coupling medium

Here, the influence of the stiffness of elastic medium on the band structure of the periodic system is investigated for the diatomic and triatomic unit cell configurations and five terms considered in the Galerkin approximation. The values of adopted parameters are the same as those in the validation study, except for the stiffness of the elastic medium. Fig. 7 shows a cross section of the band structure 3D plot for simultaneous change of the propagation constant μ and stiffness of the elastic medium k given in the horizontal axis. One can observe nine bandgaps for lower values of the stiffness parameter (white backgrounds). The first bandgap at the lowest frequency range is the narrowest while the widest one is located at the highest frequency range. The number and width of bandgaps reduces for further increase of the stiffness parameter. From the physical point of view, increasing the stiffness of the Winkler elastic medium increases the overall stiffness of the system. Different band structure can be observed in the case of triatomic unit cell configurations, where one can observe a larger number of bandgaps but with similar behavior when increasing the stiffness parameter. Moreover, Fig. 8 shows equivalent periodic systems but for the clamped-free boundary conditions on beams. This system is even more sensitive to variation of the stiffness parameter whose increase can significantly reduce the number and width of bandgaps. In the triatomic configuration case, there are initially more bangaps but their number is also reduced when increasing the stiffness parameter. Narrow and lower frequency bandgaps can be easily eliminated by increasing the stiffness parameter. The overall characteristic of all presented examples is that transmission bands are very narrow at higher frequencies.

4.4. The effect of concentrated masses

The effect of concentrated masses on dispersion curves of the periodic system of elastically connected beams in diatomic and triatomic unit cell configurations is investigated in this sub-section for five terms in Galerkin approximation. Beams in the unit cell have different cross sectional areas like in the previous examples. The values of parameters are adopted the same as in the validation study except for the values of concentrated masses. The main reason for introducing the concentrated masses is possibility to change the mass distribution and therefore the band structure of the periodic system without changing its geometrical properties. In this analysis, figures are also obtained as a cross section i.e. dispersion surface of a 3D plot obtained by changing the propagation constant μ and values of the attached point masses M_p (horizontal axis).Therefore, Fig. 9 shows the effect of change of concentrated masses on the band structure of the proposed periodic system for simply supported beams. One can observe nine bandgaps (white surfaces) for lower values of masses, including the zero-frequency bandgap. Similar to the previous examples, lower frequency bandgaps are narrower, while those at higher frequencies are wider. An increase of mass decreases the bandgaps' width while the zero-frequency bandgap vanishes. In addition, all the remaining bandgaps are shifted towards lower frequencies due to the well known feature of beam-mass systems that an increase of values of concentrated masses reduces the values of natural frequencies. Similar behaviour can be noticed in both periodic systems with diatomic and the triatomic unit cell configurations, except the latter has greater number of bandgaps. Furthermore, similar tendencies in the band structure behaviour can be observed in Fig. 10 for the same system but with the cantilever beams. In the case of small values of concentrated masses there are six bandgaps including the zero-frequency bandgap. The narrowest bandgap is at the lowest, while the widest is at the highest frequency. However, an

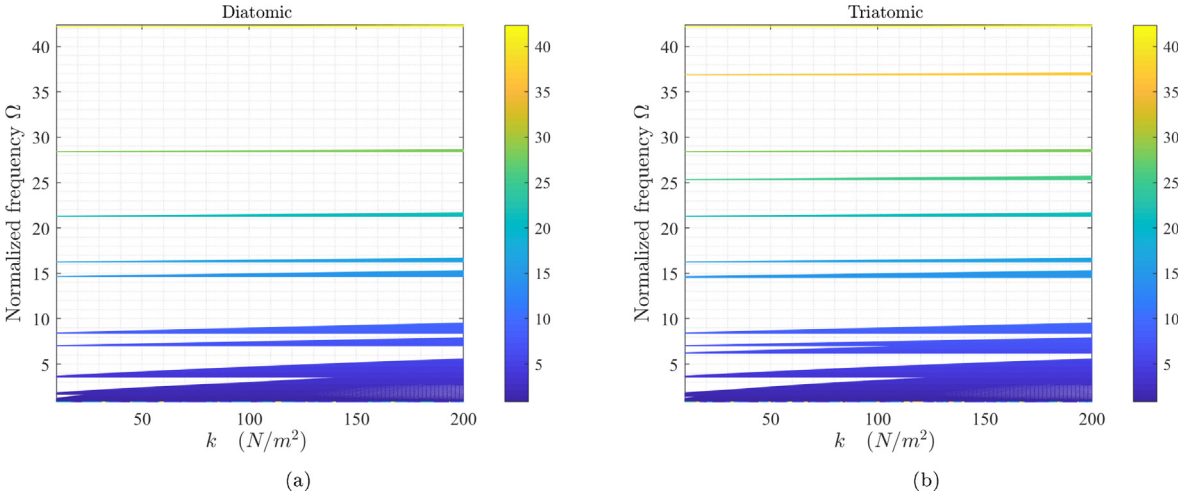

Fig. 7. The cross section of 3D frequency band structure diagrams for five terms in the Galerkin approximation and diatomic and triatomic unit cell configurations with simply supported beams. The surfaces are obtained by solving the eigenvalue problem from Eq. (29) and by changing the propagation constant μ and the stiffness of elastic coupling medium k.

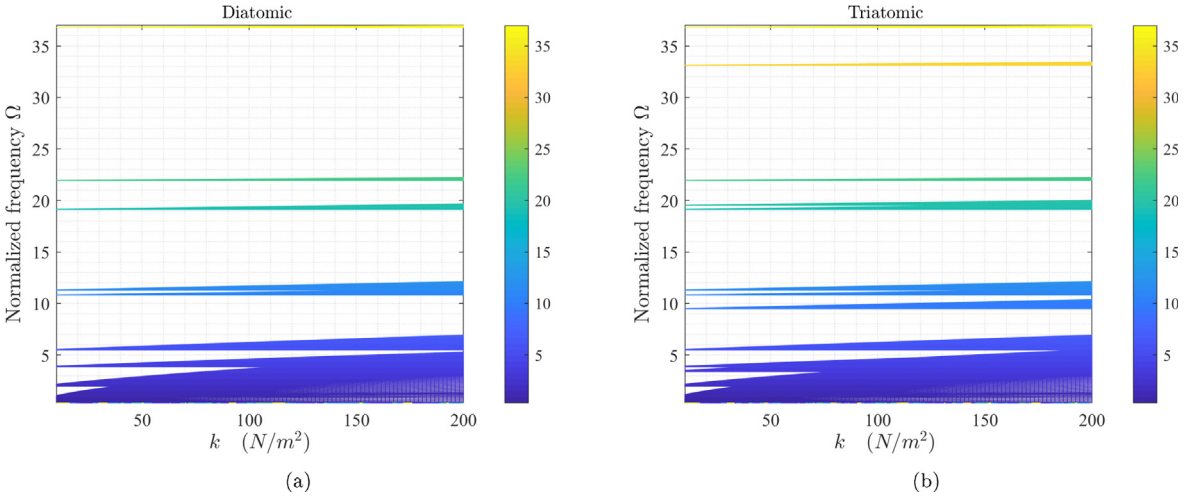

Fig. 8. The cross section of 3D frequency band structure diagrams for five terms in the Galerkin approximation and diatomic and triatomic unit cell configurations with clamped-free beams. The surfaces are obtained by solving the eigenvalue problem from Eq. (29) and by changing the propagation constant μ and the stiffness of elastic coupling medium k.

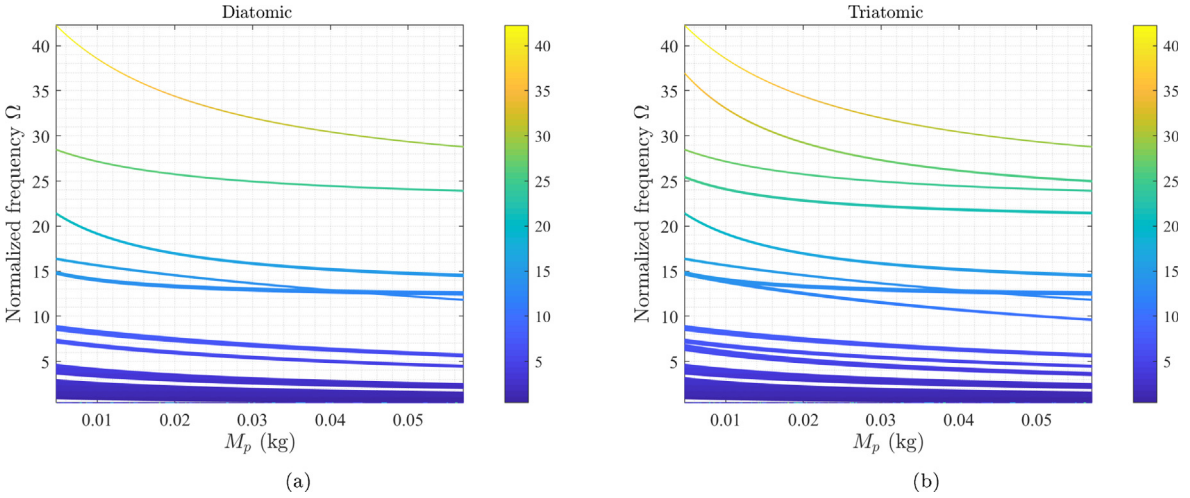

Fig. 9. The cross section of 3D frequency band structure diagrams for five terms in Galerkin approximation and diatomic and triatomic unit cell configurations with simply supported beams. The surfaces are obtained by solving the eigenvalue problem from Eq. (29) and by changing the propagation constant μ and the stiffness of elastic coupling medium M_p.

increase of the mass quickly eliminates the lowest frequency bandgaps, including the zero-frequency bandgap, and it also narrows the others. One can also notice shifting of the bandgaps towards lower values of frequency. However, in the case of triatomic configuration, the frequency ranges and the number of bandgaps for the same values of concentrated masses are different. Moreover, a veering phenomenon can be noticed in frequency dispersion plots, which is known from the literature as a point where dispersion or frequency response curves are approaching each other without crossing and then suddenly diverge one from another. Appearance of this phenomenon strongly depends on the value of concentrated masses attached to beams.

It can be outlined that the main characteristic of the proposed periodic system of elastically connected beams is that the band structure properties can be easily changed by changing the stiffness of coupling medium and values of concentrated masses attached to beams without changing the geometrical features of the system it self. The proposed model also shows the existence of the zero-frequency bandgap, which is more pronounced for the simply supported boundary conditions and certain values of concentrated masses than for the clamped-free case.

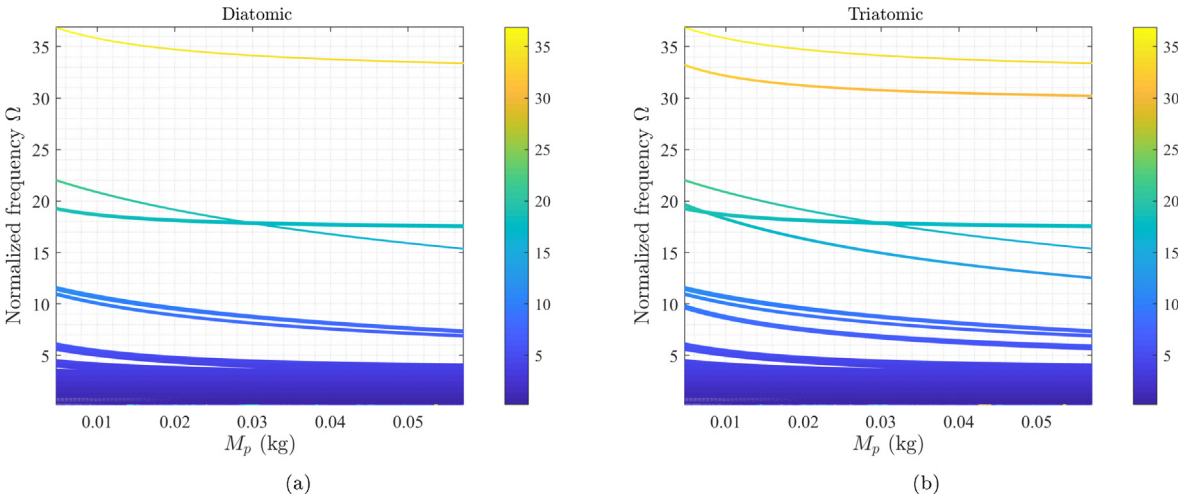

Fig. 10. The cross section of 3D frequency band structure diagrams for five terms in Galerkin approximation and diatomic and triatomic unit cell configurations with clamped-free beams. The surfaces are obtained by solving the eigenvalue problem from Eq. (29) and by changing the propagation constant μ and the stiffness of elastic coupling medium M_p.

5. Conclusions

In this work, Floquet-Bloch theorem and Galerkin approximation are suggested to study wave propagation in periodic systems based on vertically aligned and elastically connected parallel slender structures. A particular attention is devoted to the periodic system given as an array of elastically connected beams with concentrated masses and same boundary conditions. Adjacent beams are coupled through the Winkler's type of elastic medium given as uniformly distributed springs along beam's length. The eigenvalue problem is solved to determine the dispersion curves with the main assumption that the elastic wave propagates along the array of periodically repeating structures i.e. in the direction normal to the length/-surface of structural elements. The frequency band structure diagrams are validated by comparing them with the results from the finite element model and the frequency response function determined for the full model of the periodic system. Parametric study is performed to analyze the effects of different structural parameters on the frequency band structure. The following conclusions can be drawn as a result of the presented study:

- Obtained frequency band structure of the presented periodic system of elastically connected beams reveals great potential for wave attenuation applications.
- Beams boundary conditions and different unit cell configurations have shown a significant influence on the band structure diagrams of the proposed system.
- Variation of elastic medium stiffness parameter and value of concentrated masses revealed that band structure properties can be easily tuned without changing the geometrical properties of the system.

The proposed framework allows the study of more complex systems with elastically coupled structural elements such as plates or membranes. This study shows potential of the proposed periodic systems to be utilized in vibration mitigation and wave attenuation applications. Moreover, the presented model can be useful in future design of topological mechanical metamaterials based on coupled structures systems, which presents an intriguing direction for further research.

CRediT authorship contribution statement

Danilo Karličić: Conceptualization, Methodology, Software. **Milan Cajić:** Writing - original draft, Investigation, Data curation. **Stepa Paunović:** Software, Validation. **Sondipon Adhikari:** Supervision.

Declaration of Competing Interest

The authors declare that they have no known competing financial interests or personal relationships that could have appeared to influence the work reported in this paper.

Acknowledgements

D. Karličić and S. Adhikari were supported by the Marie Sklodowska-Curie Actions — - European Commission: 799201-METACTIVE. M. Cajić and S. Paunović were supported by the Serbian Ministry of Education, Science and Technological Development through the Mathematical Institute of the Serbian Academy of Sciences and Arts.

Appendix A. The mass and stiffness matrices

The mass and stiffness matrices determined in a general case are

$$\mathbf{M}_m = \begin{bmatrix} \mathbf{M}_1 & \mathbf{0} & \mathbf{0} & \mathbf{0} & \dots & \mathbf{0} \\ \mathbf{0} & \mathbf{M}_2 & \mathbf{0} & \mathbf{0} & \dots & \mathbf{0} \\ \mathbf{0} & \mathbf{0} & \mathbf{M}_3 & \mathbf{0} & \dots & \mathbf{0} \\ \dots & \dots & \dots & \mathbf{M}_i & \dots & \mathbf{0} \\ \mathbf{0} & \mathbf{0} & \mathbf{0} & \mathbf{0} & \dots & \mathbf{M}_p \end{bmatrix}_{pN\times pN},$$

$$\mathbf{K}_m = \begin{bmatrix} \mathbf{K}_1 & \mathbf{0} & \mathbf{0} & \mathbf{0} & \dots & \mathbf{0} \\ \mathbf{0} & \mathbf{K}_2 & \mathbf{0} & \mathbf{0} & \dots & \mathbf{0} \\ \mathbf{0} & \mathbf{0} & \mathbf{K}_3 & \mathbf{0} & \dots & \mathbf{0} \\ \dots & \dots & \dots & \mathbf{K}_i & \dots & \mathbf{0} \\ \mathbf{0} & \mathbf{0} & \mathbf{0} & \mathbf{0} & \dots & \mathbf{K}_p \end{bmatrix}_{pN\times pN}, \tag{30}$$

$$\mathbf{K}_{m-1} = \mathbf{K}_{m+1} = \begin{bmatrix} \mathbf{B}_1 & \mathbf{0} & \mathbf{0} & \mathbf{0} & \dots & \mathbf{0} \\ \mathbf{0} & \mathbf{B}_2 & \mathbf{0} & \mathbf{0} & \dots & \mathbf{0} \\ \mathbf{0} & \mathbf{0} & \mathbf{B}_3 & \mathbf{0} & \dots & \mathbf{0} \\ \dots & \dots & \dots & \mathbf{B}_i & \dots & \mathbf{0} \\ \mathbf{0} & \mathbf{0} & \mathbf{0} & \mathbf{0} & \dots & \mathbf{B}_p \end{bmatrix}_{pN\times pN},$$

where p is the number of the structural elements in the unit cell. The size of the matrices $(\mathbf{M}_i, \mathbf{K}_i, \mathbf{B}_i)$ inside of the global mass and stiffness matrices are related to the number of adopted terms in the Galerkin approximation N, and defined in Eq. (6).

References

[1] D. Mead, Wave propagation in continuous periodic structures: research contributions from Southampton, 1964–1995, J. Sound Vib. 190 (3) (1996) 495–524.
[2] D. Mead, A general theory of harmonic wave propagation in linear periodic systems with multiple coupling, J. Sound Vib. 27 (2) (1973) 235–260.
[3] D.J. Mead, A new method of analyzing wave propagation in periodic structures; applications to periodic Timoshenko beams and stiffened plates, J. Sound Vib. 104 (1) (1986) 9–27.
[4] D.J. Mead, The forced vibration of one-dimensional multi-coupled periodic structures: An application to finite element analysis, J. Sound Vib. 319 (1–2) (2009) 282–304.
[5] D. Mead, S. Parthan, Free wave propagation in two-dimensional periodic plates, J. Sound Vib. 64 (3) (1979) 325–348.
[6] G. Carta, M. Brun, Bloch–Floquet waves in flexural systems with continuous and discrete elements, Mech. Mater. 87 (2015) 11–26.
[7] L. Morini, M. Gei, Waves in one-dimensional quasicrystalline structures: dynamical trace mapping, scaling and self-similarity of the spectrum, J. Mech. Phys. Solids 119 (2018) 83–103.
[8] M. Nieves, G. Mishuris, L. Slepyan, Transient wave in a transformable periodic flexural structure, Int. J. Solids Struct. 112 (2017) 185–208.
[9] G. Carta, Effects of compressive load and support damping on the propagation of flexural waves in beams resting on elastic foundation, Arch. Appl. Mech. 82 (9) (2012) 1219–1232.
[10] L. Ding, H.-P. Zhu, L. Wu, Effects of axial load and structural damping on wave propagation in periodic Timoshenko beams on elastic foundations under moving loads, Phys. Lett. A 380 (31–32) (2016) 2335–2341.
[11] M. Nieves, M. Brun, Dynamic characterization of a periodic microstructured flexural system with rotational inertia, Philos. Trans. Roy. Soc. A 377 (2156) (2019) 20190113.
[12] R.K. Pal, M.I. Rosa, M. Ruzzene, Topological bands and localized vibration modes in quasiperiodic beams, New J. Phys. 21 (9) (2019) 093017.
[13] A. Piccolroaz, A. Movchan, Dispersion and localisation in structured rayleigh beams, Int. J. Solids Struct. 51 (25–26) (2014) 4452–4461.
[14] M. Gei, A. Movchan, D. Bigoni, Band-gap shift and defect-induced annihilation in prestressed elastic structures, J. Appl. Phys. 105 (6) (2009) 063507.
[15] G. Bordiga, L. Cabras, D. Bigoni, A. Piccolroaz, Free and forced wave propagation in a rayleigh-beam grid: flat bands, dirac cones, and vibration localization vs isotropization, Int. J. Solids Struct. 161 (2019) 64–81.
[16] J.M. De Ponti, A. Colombi, R. Ardito, F. Braghin, A. Corigliano, R.V. Craster, Graded elastic metasurface for enhanced energy harvesting, New J. Phys. 22 (1) (2020) 013013.
[17] Z. Cheng, W. Lin, Z. Shi, Wave dispersion analysis of multi-story frame building structures using the periodic structure theory, Soil Dyn. Earthquake Eng. 106 (2018) 215–230.
[18] S. Gonella, M. Ruzzene, Homogenization and equivalent in-plane properties of two-dimensional periodic lattices, Int. J. Solids Struct. 45 (10) (2008) 2897–2915.
[19] D. Torrent, J. Sánchez-Dehesa, Acoustic resonances in two-dimensional radial sonic crystal shells, New J. Phys. 12 (7) (2010) 073034.
[20] S. Hajarolasvadi, A.E. Elbanna, Dynamics of metamaterial beams consisting of periodically-coupled parallel flexural elements: a theoretical study, J. Phys. D: Appl. Phys. 52 (31) (2019) 315101.

[21] O. Avila-Pozos, A. Movchan, S. Sorokin, Propagation of elastic waves along interfaces in layered beams, in: IUTAM Symposium on Asymptotics, Singularities and Homogenisation in Problems of Mechanics, Springer, 2003, pp. 53–61.
[22] M. Ruzzene, F. Scarpa, Control of wave propagation in sandwich beams with auxetic core, J. Intell. Mater. Syst. Struct. 14 (7) (2003) 443–453.
[23] M. Serpilli, S. Lenci, Asymptotic modelling of the linear dynamics of laminated beams, Int. J. Solids Struct. 49 (9) (2012) 1147–1157.
[24] H. Saito, H. Tani, Vibrations of bonded beams with a single lap adhesive joint, J. Sound Vib. 92 (2) (1984) 299–309.
[25] W. Brito, C. Maia, A. Mendonca, Bending analysis of elastically connected euler–bernoulli double-beam system using the direct boundary element method, Appl. Math. Model. 74 (2019) 387–408.
[26] S. Paunović, M. Cajić, D. Karličić, M. Mijalković, Dynamics of fractional-order multi-beam mass system excited by base motion, Appl. Math. Model. 80 (2020) 702–723.
[27] D. Karličić, M. Cajić, S. Adhikari, P. Kozić, T. Murmu, Vibrating nonlocal multi-nanoplate system under inplane magnetic field, Eur. J. Mech. A/Solids 64 (2017) 29–45.
[28] P. Martinsson, A. Movchan, Vibrations of lattice structures and phononic band gaps, Q. J. Mech. Appl. Mech. 56 (1) (2003) 45–64.
[29] M.I. Hussein, M.J. Leamy, M. Ruzzene, Dynamics of phononic materials and structures: Historical origins, recent progress, and future outlook, Appl. Mech. Rev. 66 (4) (2014) 040802.
[30] H. Peng, P.F. Pai, Acoustic metamaterial plates for elastic wave absorption and structural vibration suppression, Int. J. Mech. Sci. 89 (2014) 350–361.
[31] M.I. Rosa, R.K. Pal, J.R. Arruda, M. Ruzzene, Edge states and topological pumping in spatially modulated elastic lattices, Phys. Rev. Lett. 123 (3) (2019) 034301.
[32] R.F. Boukadia, C. Droz, M.N. Ichchou, W. Desmet, A bloch wave reduction scheme for ultrafast band diagram and dynamic response computation in periodic structures, Finite Elem. Anal. Des. 148 (2018) 1–12.
[33] M. Sigalas, E. Economou, Elastic waves in plates with periodically placed inclusions, J. Appl. Phys. 75 (6) (1994) 2845–2850.
[34] L. Han, Y. Zhang, Z.-Q. Ni, Z.-M. Zhang, L.-H. Jiang, A modified transfer matrix method for the study of the bending vibration band structure in phononic crystal euler beams, Physica B 407 (23) (2012) 4579–4583.
[35] V. Laude, R.P. Moiseyenko, S. Benchabane, N.F. Declercq, Bloch wave deafness and modal conversion at a phononic crystal boundary, AIP Adv. 1 (4) (2011) 041402.
[36] M.I. Hussein, G.M. Hulbert, R.A. Scott, Dispersive elastodynamics of 1d banded materials and structures: analysis, J. Sound Vib. 289 (4–5) (2006) 779–806.
[37] L. Junyi, D. Balint, An inverse method to determine the dispersion curves of periodic structures based on wave superposition, J. Sound Vib. 350 (2015) 41–72.
[38] G. Shmuel, R. Band, Universality of the frequency spectrum of laminates, J. Mech. Phys. Solids 92 (2016) 127–136.
[39] C. Sugino, S. Leadenham, M. Ruzzene, A. Erturk, On the mechanism of bandgap formation in locally resonant finite elastic metamaterials, J. Appl. Phys. 120 (13) (2016) 134501.
[40] A. Casalotti, S. El-Borgi, W. Lacarbonara, Metamaterial beam with embedded nonlinear vibration absorbers, Int. J. Non-Linear Mech. 98 (2018) 32–42.
[41] E.E. Basta, M. Ghommem, S.A. Emam, Vibration suppression and optimization of conserved-mass metamaterial beam, Int. J. Non-Linear Mech. 120 (2020) 103360.
[42] C. Sugino, Y. Xia, S. Leadenham, M. Ruzzene, A. Erturk, A general theory for bandgap estimation in locally resonant metastructures, J. Sound Vib. 406 (2017) 104–123.
[43] Y. Xiao, J. Wen, X. Wen, Longitudinal wave band gaps in metamaterial-based elastic rods containing multi-degree-of-freedom resonators, New J. Phys. 14 (3) (2012) 033042.
[44] Z. Liu, X. Zhang, Y. Mao, Y. Zhu, Z. Yang, C.T. Chan, P. Sheng, Locally resonant sonic materials, Science 289 (5485) (2000) 1734–1736.
[45] R. Zhu, G. Huang, G. Hu, Effective dynamic properties and multi-resonant design of acoustic metamaterials, J. Vib. Acoust. 134 (3) (2012) 031006.
[46] L. Raghavan, A.S. Phani, Local resonance bandgaps in periodic media: Theory and experiment, J. Acoust. Soc. Am. 134 (3) (2013) 1950–1959.
[47] Y. Xiao, J. Wen, G. Wang, X. Wen, Theoretical and experimental study of locally resonant and bragg band gaps in flexural beams carrying periodic arrays of beam-like resonators, J. Vib. Acoust. 135 (4) (2013) 041006.
[48] L. Liu, M.I. Hussein, Wave motion in periodic flexural beams and characterization of the transition between bragg scattering and local resonance, J. Appl. Mech. 79 (1) (2012) 011003.
[49] Y. Achaoui, T. Antonakakis, S. Brûlé, R. Craster, S. Enoch, S. Guenneau, Clamped seismic metamaterials: ultra-low frequency stop bands, New J. Phys. 19 (6) (2017) 063022.
[50] D. Bigoni, A. Movchan, Statics and dynamics of structural interfaces in elasticity, Int. J. Solids Struct. 39 (19) (2002) 4843–4865.
[51] M. Brun, S. Guenneau, A.B. Movchan, D. Bigoni, Dynamics of structural interfaces: filtering and focussing effects for elastic waves, J. Mech. Phys. Solids 58 (9) (2010) 1212–1224.
[52] P. Hagedorn, A. DasGupta, Vibrations and waves in continuous mechanical systems, Wiley Online Library, 2007.
[53] C. Kittel, P. McEuen, P. McEuen, Introduction to solid state physics, vol. 8, Wiley, New York, 1996.
[54] T. Chatterjee, D. Karličić, S. Adhikari, M.I. Friswell, Gaussian process assisted stochastic dynamic analysis with applications to near-periodic structures, Mech. Syst. Signal Process. 149 (2021) 107218.